Hydrogen Bond Lifetimes and Clustering of Methanol in Carbon Tetrachloride Solutions

K. Bloch and C. P. Lawrence*

Department of Chemistry, Grand Valley State University, Allendale, Michigan 49401

Received: July 24, 2009; Revised Manuscript Received: November 13, 2009

NMR experiments and ab initio calculations suggest that methanol forms small cyclic hydrogen bond clusters (4−6 molecules) in the condensed phase. In contrast, molecular dynamics simulations have indicated that methanol will form large branched chains that extend to include hundreds of molecules. In this paper, we performed a series of simulations examining the structure and dynamics of methanol/carbon tetrachloride mixtures. We show that two simulation models are capable of reproducing the trends in the experimental NMR data despite the fact that they indicate that the structure of the liquid is dominated by large branched chains. We hypothesize that the experimental results can be described by variations in the hydrogen bond lifetime with methanol concentration.

1. Introduction

Hydrogen bonding liquids have an unparalleled significance in chemistry and biochemistry, ranging from the unique properties of water[1−5] to their role in the structures of biomolecules.[6−9] Despite their importance, the depth of our understanding of the structure and dynamics of these fluids is unsatisfactory. While liquid water is clearly the most significant of these, the fact that it can form up to four hydrogen bonds provides for a fairly complicated system despite the paucity of atoms. Instead, small aliphatic alcohols are often used to study hydrogen bonding dynamics because they tend to form just two hydrogen bonds per molecule.[10−20] In this case, it is expected that each molecule will be involved in only two hydrogen bonds, one in which it is the donor of the hydrogen atom and another in which it is the acceptor.

While it is understood that methanol will form a hydrogen bond network of some form in the condensed phase, it is not possible to probe the structure of that network directly. In contrast, in the gas phase, the cluster size can be determined unambiguously. Both infrared spectroscopy[21−23] and ab initio calculations[23−27] conclude that these gas-phase clusters consist primarily of cyclic species ranging in size from three to six molecules.

In the liquid phase, Sarkar and Joarder attempted to model their neutron scattering data of pure methanol by assuming that the molecules were arranged in either tetramer rings, tetramer chains, or hexamer rings.[28] They found that the best agreement came by assuming hexamer rings, while the poorest agreement resulted with tetramer chains.

Wendt and Farrar tackled the problem in a set of NMR experiments using mixtures of methanol and carbon tetrachloride.[17] In those experiments, they measured the spin-lattice relaxation time and chemical shift of the alcohol, from which they were able to determine the rotational correlation time. They found that at very low methanol concentration, the correlation time was quite small. It rose quickly with concentration until reaching a maximum at a mole fraction of 0.5. They hypothesized that the variation in the rotational correlation time was the result of a shift in the cluster size as the concentration changed (at a mole fraction of 0.5, the system forms larger clusters on average than at other concentrations). From the rotational correlation time and the measured viscosity of the solutions, they estimated that the average volume of the hydrogen-bonded clusters corresponded to about midway between that of a cyclic pentamer and a cyclic hexamer.

In contrast to the conclusions drawn from these experiments, molecular simulations indicate a tendency to form large, branched chains.[29−32] In pure methanol, these chains are found to average between 15 and 20 molecules, with some incorporating hundreds of molecules. These models are fairly successful in reproducing the experimentally observed structure of the liquid (as measured by X-ray or neutron diffraction),[33] although it should be noted that these experiments do not directly distinguish between rings and chains. Matsumoto and Gubbins examined several dynamical properties associated with the number of hydrogen bonds in which a molecule participates.[34] They found that in pure methanol, the majority of the molecules have two hydrogen bonds and that this state has the longest lifetime.

In this paper, we employed multiple molecular simulation models to examine the rotational dynamics of methanol in carbon tetrachloride. We found that two of the three models concur with the experimental observations regarding a maximum in the correlation time. We then examined the nature of the clustering of the methanol molecules in those two models.

2. Simulation Methods

We examined the rotational dynamics of three separate models. Model I consisted of the OPLS model for methanol[30] and the carbon tetrachloride model developed by McDonald et al.[35] In this case, the methyl group of methanol was treated as a unified atom and all of the atoms were held rigid. Model II employed the same carbon tetrachloride model but used a more recent model for methanol (the TraPPE-UA model).[36] As implied by the UA notation, this model also employed a unified atom for the methyl group. However, in this case, the molecules were flexible. As the model for carbon tetrachloride was originally devised for a rigid system, an intramolecular force field was included. The force constants were obtained by stretching the internal coordinates in a B3LYP/6-31G(d) calculation. For the bond stretches and bending motions, the force constants were found to be 291 J/m^2 and 2.03 × 10^{-22} J/deg^2,

* To whom correspondence should be addressed.

10.1021/jp907079s
Published on Web 12/17/2009

respectively. Both models I and II employed constant charges on the atoms for the intermolecular forces. In model III, the charges were allowed to fluctuate based on their external environment.[33,37] The methanol in this case employed interaction sites for all six atoms, and both molecules were held rigid.

Cubic periodic boundary conditions were applied, and the electrostatic forces were calculated using the damped shifted force alternative to the Ewald summation as described by Fennell and Gezelter.[38−40] The damping parameter, α, was 0.2 Å^{-1}, and the cutoff radius was set to half of the box length. The equations of motion were integrated using the leapfrog algorithm with a time step of 0.5 fs. For each of the different systems, during both the equilibration and production runs, the temperature was held constant at 300 K through velocity scaling at each step. For the fluctuating charge model, the nuclear degrees of freedom were maintained at 300 K, but the temperature for the electrostatic degrees of freedom were maintained at 5 K.[41] By doing so, the charges remained near the values that minimize the electrostatic energy, but they were still able to adjust rapidly to the changes in the atomic positions. In each simulation, a total of 500 molecules was used, with the mole fraction of methanol ranging from 0.002 (a single alcohol molecule) to pure methanol. The density of the system was set to the experimentally measured value for that particular concentration at 300 K,[42] and the molecules were regularly arranged in a cubic box. Velocities were assigned randomly to each atom. The system was then equilibrated for 40 ps, followed by a subsequent run of 250 ps.

3. Results and Discussion

Veldhuizen and Leeuw examined the thermodynamic properties of model I, although their simulation was done at constant pressure.[43] Experimentally, the excess enthalpy (the difference between the enthalpy of the mixture and the weighted sum of the enthalpies of the two pure liquids) was found to peak at low methanol concentration (about $x_{MeOH} = 0.3$). The simulation predicted a maximum excess enthalpy at $x_{MeOH} = 0.5$ with a value of about twice that of the experiment. In our constant volume simulations, we found very similar results with model II and that model III predicts an even higher excess enthalpy.

The rotational correlation time is given by integrating the second-rank rotational time correlation function

$$\tau = \int_0^\infty \mathrm{d}t \langle P_2(\hat{u}(t)\cdot\hat{u}(0))\rangle \qquad (1)$$

where $\hat{u}$ is the unit vector along the OH bond of the methanol molecule and P_2 is the second Legendre polynomial.[44] The calculated rotational correlation time for models I, II, and III and the corresponding experimental data[17] are shown in Figure 1. As this data shows, for model I, there is no significant maximum in the computational results. Both models II and III, however, have maxima at a methanol mole fraction of 0.3, with model II providing better overall agreement with the experimentally observed trend and near-quantitative agreement at low methanol concentration.

While it has been shown previously that the methanol molecules in model I have a strong preference toward the formation of long chains at the expense of cyclic structures,[29−32] it is unknown whether models II and III do as well. Thus, we examined the clustering in those models here. In our examination of hydrogen bonding, a hydrogen bond was defined as having an oxygen−oxygen distance and an oxygen−hydrogen distance less than their respective minima in their pair correlation functions. While it is more common that an angular criterion is used in place of the oxygen−hydrogen distance, they do serve the same purpose − restricting hydrogen bonds to be relatively linear.[45−47] In Table 1, we summarize our findings regarding the clustering of the methanol molecules. We considered a chain to involve three or more methanol molecules where dimers were counted as a separate category. Our definition of a chain included branching structures resulting from molecules that have more than two hydrogen bonds as well. In model II, at a cluster size of about 15 molecules, there are equal numbers of branched and linear chains. By cluster sizes of about 30 molecules, the vast majority of the chains have one or more branches. A similar statement can be made about model III; however, the turning points were 9 and 20 molecules, respectively. A ring, however, involved only molecules with two hydrogen bonds. While it is conceivable that a ring could be branched by containing a molecule that has three hydrogen bonds, this was only observed in molecules that were part of a much larger chain and were thus classified as chains. Using the TraPPE force field from model II, Stubbs and Siepmann examined clustering in dilute solutions of 1-hexanol in *n*-hexane.[48] For cluster sizes between 4 and 6 molecules, they found roughly equal numbers of rings and linear chains. At low concentrations, we find that these numbers are roughly equal in our system as well. However, we observed fewer branched structures at those concentrations than were found in 1-hexanol.

When a hydrogen bond forms in model III, the fluctuating charges respond to the external electric field by increasing the polarity of the OH bonds. Should a second hydrogen bond form to the same molecule, the bond polarity increases further, leading to an increase in the strength of the hydrogen bonds. Thus, model III would be expected to emphasize cooperativity in hydrogen bonding, which is cited as the driving force behind the formation of rings in the gas phase. However, we observed very few rings at all concentrations. It has been observed that polarizable models such as model III underestimate the increase

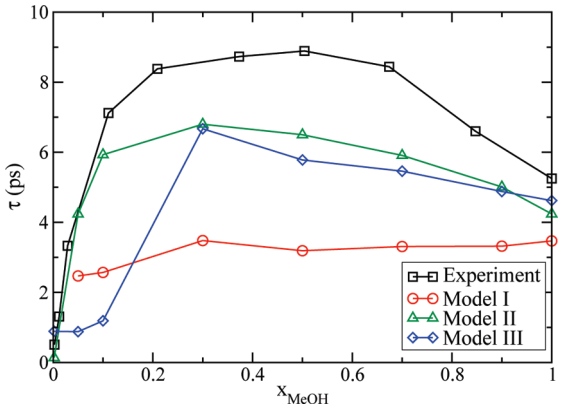

Figure 1. Rotational correlation time as a function of methanol concentration. The experimental data is from Wendt and Farrar.[17]

TABLE 1: Fraction of Molecules in Various Hydrogen Bonding States

	model II				model III			
x_{MeOH}	monomer	dimer	chain	ring	monomer	dimer	chain	ring
0.05	14.5	14.1	41.4	30.0	91.6	6.6	1.7	0.0
0.1	6.3	5.3	24.8	63.6	66.9	17.4	15.1	0.5
0.3	1.1	2.0	66.2	30.7	8.6	3.7	84.7	3.0
0.5	0.7	0.9	86.5	11.8	5.9	4.4	85.8	3.9
0.7	0.7	0.8	91.8	6.6	3.8	3.5	91.8	0.9
0.9	0.5	0.8	93.1	5.5	1.9	2.4	94.8	0.9
1.0	0.5	0.8	93.1	5.6	1.4	1.7	95.7	1.3

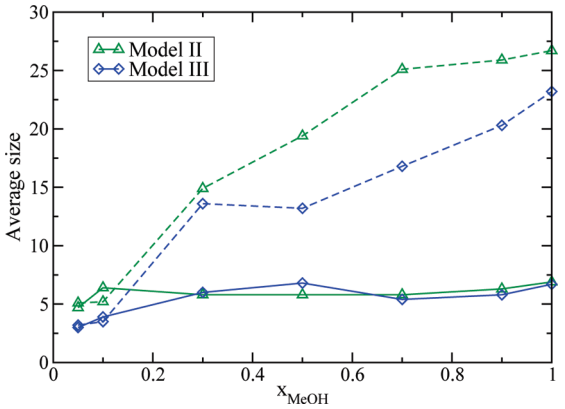

Figure 2. Average number of methanol molecules in rings (solid lines) and chains (dashed lines) for models II and III.

in the dipole moment of molecules in gas-phase clusters. That is, the cooperative effect is in the model but not as strong as it ought to be.[49,50] In contrast, model II (which has constant charges but flexible bonds) showed that cyclic structures were quite significant at low methanol concentration and were the most dominant structure at $x_{MeOH} = 0.1$. While this latter result initially appears to provide support for the hypothesis posed by Wendt and Farrar,[17] the maximum in the number of rings does not correspond to the maximum in the rotational correlation time (which occurs at $x_{MeOH} = 0.3$), and in model III, a maximum in τ is observed without the formation of rings.

As the number of methanol molecules in the rings and chains does not correlate with τ, we next considered the possibility that the size of the clusters does. In Figure 2, we see that for both models, there is little change in the average size of the rings that do form and that the chain size increases monotonically with methanol concentration.

Matsumoto and Gubbins found that in pure methanol, the fewer hydrogen bonds the molecule formed, the faster it was able to reorient.[34] It was also found that while the vast majority of methanol molecules have two hydrogen bonds, the average molecule reoriented significantly faster than those with two hydrogen bonds. With that in mind, we examined the hydrogen bond lifetime as the methanol concentration changed. To calculate this lifetime, we tracked the amount of time between the formation of a new hydrogen bond and the breaking of that bond. The average lifetime is compared to τ for models II and III in Figure 3. For model III, the correlation between these two quantities is very strong, with a sharp maximum at $x_{MeOH} = 0.3$. For model II, there is also a maximum hydrogen bond lifetime at $x_{MeOH} = 0.3$ that corresponds to the peak in τ, although the correlation is weaker.

This trend in the hydrogen bond lifetime, in turn, is dictated by the strength of the bonds which are shown in Figure 4. For both models II and III, the hydrogen bond strength peaks at $x_{MeOH} = 0.3$. As the concentration approaches pure methanol, the strength of this interaction falls by 0.6 kJ/mol in model II and 1.0 kJ/mol in model III. Assuming that the rate of breaking of these bonds followed an Arrhenius behavior, at 300 K, we would anticipate a reduction in this rate of 21 and 33% as the mole fraction increases from $x_{MeOH} = 0.3$ to 1 for models II and III, respectively. In comparison, the observed changes in the hydrogen bond lifetimes are 26% for model II and 28% for model III. For model II, we see a decline of similar magnitude as the concentration of methanol is reduced below $x_{MeOH} = 0.3$, which corresponds to the more modest decline in the hydrogen

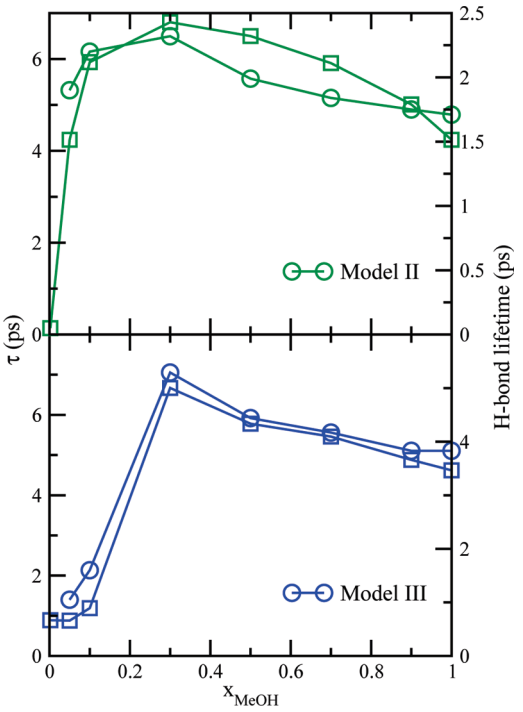

Figure 3. The rotational correlation time (squares) and the hydrogen bond lifetime (circles) as a function of methanol concentration for models II and III.

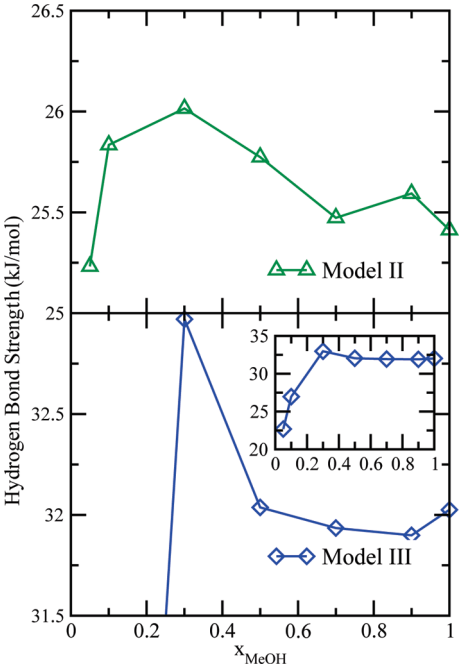

Figure 4. Average hydrogen bond strength as a function of methanol concentration for models II and III. For model III, the data is shown on the same scale as model II to emphasize the peak at $x_{MeOH} = 0.3$. At concentrations below $x_{MeOH} = 0.3$, the strength falls off dramatically, as shown in the inset.

bond lifetime and, thereby, the rotational correlation time. In contrast, there is a tremendous drop in the hydrogen bond strength in model III at mole fractions less than 0.3. This leads to hydrogen bonds that break readily and a rotational correlation time that is only slightly different from the value obtained at infinite dilution.

TABLE 2: Fraction of Molecules with a Given Number of Hydrogen Bonds

	model II				model III			
x_{MeOH}	$n_{HB} = 0$	$n_{HB} = 1$	$n_{HB} = 2$	$n_{HB} = 3$	$n_{HB} = 0$	$n_{HB} = 1$	$n_{HB} = 2$	$n_{HB} = 3$
0.05	14.5	28.8	55.1	1.6	91.6	7.7	0.7	0.0
0.1	6.3	14.6	76.0	3.1	66.9	26.1	6.8	0.2
0.3	1.1	10.3	83.1	5.5	8.6	17.7	65.1	8.5
0.5	0.7	10.6	82.1	6.4	5.9	18.5	65.5	10.0
0.7	0.7	10.1	82.9	6.3	3.8	18.4	67.2	10.5
0.9	0.5	10.3	82.1	7.0	1.9	17.1	68.8	12.2
1.0	0.5	10.4	81.8	7.3	1.4	15.8	70.3	12.4

To understand this variation in the hydrogen bond strength, we once again turned to the work of Matsumoto and Gubbins.[34] In that paper, they noted that the hydrogen bond strength was substantially weaker for molecules that have one or three hydrogen bonds than for those that have two (a difference of about 1 kJ/mol). The fraction of methanol molecules with varying numbers of hydrogen bonds are shown in Table 2. For model II, at low concentration, there are relatively few hydrogen bonds overall, which, in turn, results in a larger number of dimers and short chains and a larger fraction of molecules with a single hydrogen bond. As the concentration rises, the number of dimers diminishes, and the chain size increases, leading to a greater proportion of molecules in the more stable two-hydrogen-bond state. At high concentration, however, the number of molecules that have three hydrogen bonds begins to rise, leading to an overall decrease in the hydrogen bond stability. The trend is similar for model III; however, there is no decline in the number of molecules with two hydrogen bonds at high concentrations. In model III, the strength of the hydrogen bonds falls off far more sharply when a third bond is formed. This drop was sufficient to lead to an overall decrease in the hydrogen bond strength. It also appears that this sharp drop in strength for model III is responsible for the fact that model III has a much higher average hydrogen bond strength than model II but a similar hydrogen bond lifetime.

5. Conclusion

We have shown that two different simulation models are able to reproduce the experimental observation of a maximum in the rotational correlation time. In both cases, the calculated correlation times are smaller than those measured experimentally, and the maximum appears at a lower methanol concentration, but the best agreement came with the TraPPE-UA model (model II) for methanol. As the fluctuating charge model (model III) is parametrized for the simulation of pure methanol, it seems to exaggerate the cooperativity of hydrogen bonding. As such, at low concentration when there is less cooperativity, the hydrogen bonds are far weaker. While the agreement between the experiments and the simulations is less than perfect, the most significant conclusion from this work is that the simulations do have a maximum in τ, but that maximum does not correspond to the size or distribution of hydrogen-bonded clusters. We therefore hypothesize that the slow rotations at moderate methanol concentration are due to an increase in the average lifetime of the hydrogen bonds, which is tied to the fraction of methanol molecules that have two hydrogen bonds. This increase in hydrogen bond strength does have a loose connection to the structure of the hydrogen-bonded liquid in that the maximum in the hydrogen bond strength corresponds to a maximum in the number of methanol molecules that have two hydrogen bonds.

Acknowledgment. We are grateful for generous support from the Petroleum Research Fund through Grant PRF# 44874-GB 6.

References and Notes

(1) Franks, F. Ed. *Water: A Comprehensive Treatise*; Plenum Press: New York, 1972; Vol. 1.
(2) Eisenberg, D.; Kauzmann, W. *The Structure and Properties of Water*; Oxford University Press: New York, 1969.
(3) Dorsey, N. E. *Properties of Ordinary Water-Substance*; Reinhold: New York, 1940.
(4) *Water and Aqueous Solutions: Structure, Thermodynamics and Transport Processes*; Horne, R. A., Ed.; Wiley: New York, 1972.
(5) *The Hydrogen Bond: Recent Developments in Theory and Experiments*; Schuster, P., Zundel, G., Sandorfy, C., Eds.; North-Holland: Amsterdam, 1976; Vol. 1−3.
(6) Kendrew, J. C.; Dickerson, R. E.; Standberg, B. E.; Hart, R. G.; Davies, D. R.; Phillips, D. C.; Shore, V. C. *Nature* **1960**, *185*, 422.
(7) Clore, G. M.; Gronenborn, A. M. *Annu. Rev. Biophys. Biophys. Chem.* **1991**, *20*, 29.
(8) Stryer, L. *Annu. Rev. Biochem.* **1978**, *47*, 819.
(9) Wang, T.; Du, D.; Gai, F. *Chem. Phys. Lett.* **2003**, *370*, 842.
(10) Liddel, U.; Becker, E. D. *Spectrochim. Acta* **1957**, *10*, 70.
(11) Graener, H.; Ye, T. Q.; Laubereau, A. *J. Chem. Phys.* **1989**, *90*, 3413.
(12) Graener, H.; Ye, T. Q.; Laubereau, A. *J. Chem. Phys.* **1989**, *91*, 1043.
(13) Woutersen, S.; Emmerichs, U.; Bakker, H. J. *J. Chem. Phys.* **1997**, *107*, 1483.
(14) Laenen, R.; Rauscher, C. *J. Chem. Phys.* **1997**, *106*, 8974.
(15) Laenen, R.; Rauscher, C. *J. Chem. Phys.* **1997**, *107*, 9759.
(16) Wendt, M. A.; Meiler, J.; Weinhold, F.; Farrar, T. C. *Mol. Phys.* **1998**, *93*, 145.
(17) Wendt, M. A.; Farrar, T. C. *Mol. Phys.* **1998**, *95*, 1077.
(18) Wendt, M. A.; Zeidler, M. D.; Farrar, T. C. *Mol. Phys.* **1999**, *97*, 753.
(19) Ferris, T. D.; Zeidler, M. D.; Farrar, T. C. *Mol. Phys.* **2000**, *98*, 737.
(20) Murdoch, K. M.; Ferris, T. D.; Wright, J. C.; Farrar, T. C. *J. Chem. Phys.* **2002**, *116*, 5717.
(21) van Thiel, M.; Becker, E. D.; Pimentel, G. C. *J. Chem. Phys.* **1957**, *27*, 95.
(22) Huisken, F.; Kaloudis, M.; Koch, M.; Werhahn, O. *J. Chem. Phys.* **1996**, *105*, 8965.
(23) Provencal, R. A.; Paul, J. B.; Roth, K.; Chapo, C.; Casaes, R. N.; Saykally, R. J.; Tschumper, G. S.; Schaefer, H. F., III *J. Chem. Phys.* **1999**, *110*, 4258.
(24) Mó, O.; Yanez, M.; Elguero, J. *J. Chem. Phys.* **1997**, *107*, 3592.
(25) Buck, U.; Siebers, J. G. *Eur. Phys. J. D* **1998**, *1*, 207.
(26) Buck, U.; Siebers, J. G.; Wheatley, R. J. *J. Chem. Phys.* **1998**, *108*, 20.
(27) Hagemeister, F. C.; Gruenloh, C. J.; Zwier, T. S. *J. Phys. Chem. A* **1998**, *102*, 82.
(28) Sarkar, S.; Joarder, R. N. *J. Chem. Phys.* **1993**, *99*, 2032.
(29) Jorgensen, W. L. *J. Am. Chem. Soc.* **1981**, *103*, 335.
(30) Jorgensen, W. L. *J. Phys. Chem.* **1986**, *90*, 1276.
(31) Haughney, M.; Ferrario, M.; McDonald, I. R. *J. Phys. Chem.* **1987**, *91*, 4934.
(32) Gao, J. L.; Habibollazadeh, D.; Shao, L. *J. Phys. Chem.* **1995**, *99*, 16460.
(33) Patel, S.; Brooks, C. L., III *J. Chem. Phys.* **2005**, *122*, 024508.
(34) Matsumoto, M.; Gubbins, K. E. *J. Chem. Phys.* **1990**, *93*, 1981.
(35) McDonald, I. R.; Bounds, D. G.; Klein, M. L. *Mol. Phys.* **1982**, *45*, 521.
(36) Chen, B.; Potoff, J. J.; Siepmann, J. I. *J. Phys. Chem. B* **2001**, *105*, 3093.
(37) Masia, M.; Probst, M.; Rey, R. *J. Chem. Phys.* **2004**, *121*, 7362.
(38) Fennell, C. J.; Gezelter, J. D. *J. Chem. Phys.* **2006**, *124*, 234104.
(39) Wolf, D.; Keblinski, P.; Phillpot, S. R.; Eggebrecht, J. *J. Chem. Phys.* **1999**, *110*, 8254.
(40) Zahn, D.; Schilling, B.; Kast, S. M. *J. Phys. Chem. B* **2002**, *106*, 10725.

(41) Rick, S. W.; Stuart, S. J.; Berne, B. J. *J. Chem. Phys.* **1994**, *101*, 6141.
(42) Paraskevopoulos, G. C.; Missen, R. W. *Trans. Faraday Soc.* **1962**, *58*, 869.
(43) Veldhuizen, R.; Leeuw, S. W. *J. Chem. Phys.* **1996**, *105*, 2828.
(44) Abragam, A. *The Principles of Nuclear Magnetism*; Oxford: London, 1961.
(45) Bertolini, D.; Cassettari, M.; Ferrario, M.; Grigolini, P.; Salvetti, G. *Adv. Chem. Phys.* **1985**, *62*, 277.
(46) Luzar, A.; Chandler, D. *Phys. Rev. Lett.* **1996**, *76*, 928.
(47) Martí, J. *J. Chem. Phys.* **1999**, *110*, 6876.
(48) Stubbs, J. M.; Siepmann, J. I. *J. Phys. Chem. B* **2002**, *106*, 3968.
(49) Chen, B.; Xing, J.; Siepmann, J. I. *J. Phys. Chem. B* **2000**, *104*, 2391.
(50) Chen, B.; Siepmann, J. I.; Klein, M. L. *J. Phys. Chem. A* **2005**, *109*, 1137.

JP907079S